Available online at www.sciencedirect.com
SCIENCE DIRECT
Coordination Chemistry Reviews 250 (2006) 1792–1803
COORDINATION CHEMISTRY REVIEWS
www.elsevier.com/locate/ccr

Review

Photophysics and photochemistry of kinetically labile, water-soluble porphyrin complexes

Ottó Horváth [a,*], Róbert Huszánk [a], Zsolt Valicsek [a], György Lendvay [a,b]

[a] *Pannon University, Department of General and Inorganic Chemistry, H-8200 Veszprém, P.O. Box 158, Hungary*
[b] *Institute of Structural Chemistry, Hungarian Academy of Sciences, H-1525 Budapest, P.O. Box 17, Hungary*

Received 5 October 2005; accepted 14 February 2006
Available online 6 March 2006

Contents

Abstract

Most metalloporphyrins contain a metal ion in the center of the planar tetrapyrrolic ring system, resulting in a kinetically inert complex. If, however, the ionic radius of the metal ions is too large (over ca. 75–80 pm) to fit into the hole in the center of the macrocycle, they are located out of the ligand plane, distorting it. These kinetically labile sitting-atop (SAT) complexes display characteristic structural and photoinduced properties that strongly deviates from those of the regular metalloporphyrins. In this paper we review the results of studies on water-soluble $TPPS^{6-}$ (H_2TPPS^{4-} = 5,10,15,20-tetrakis(4-sulfonatophenyl)porphyrin anion) complexes of some metal ions, each with two different oxidation states (Fe^{3+}, Fe^{2+}, Tl^{3+}, Tl^{+}, Hg^{2+}, and Hg_2^{2+}) performed in order to reveal how the charge, and especially the size of the metal center influence their composition, structure and photoinduced behavior. While the heme-like (1:1) iron(II) complex displays typical SAT properties (red-shifted Soret absorption band and blue-shifted emission and Q absorption bands, irreversible photoinduced porphyrin ligand-to-metal charge transfer reaction), the corresponding iron(III) porphyrin is a regular one with no emission and photoredox behavior. Moreover, in the synthesis of the latter complex Fe^{2+} ions act as catalyst via formation of kinetically labile iron(II) porphyrin as intermediate. In contrast to iron, thallium (Tl^{3+}, Tl^{+}) and mercury (Hg^{2+}, Hg_2^{2+}) ions form exclusively SAT complexes, regardless of their oxidation state. These metalloporphyrins, however, are of various composition with considerable variation in the efficiencies of their emission and photoredox activities. While thallium(III) forms 1:1 $TPPS^{6-}$ complex, the composition of the corresponding thallium(I) species is 2:1. Despite their similar absorption and emission spectra, the quantum yield for the photoredox degradation of the thallium(I) complex is significantly larger, due to its much lower stability. Mercury ions (both Hg^{2+} and Hg_2^{2+}) form also bis-porphyrin complexes, which are, however, not fluorescent at room temperature. Interestingly, the energy of the Q-band excitation is enough to promote their photoinduced dissociation, which can only be observed upon Soret-band irradiation in the case of the monoporphyrin complexes. All these results clearly indicate that the photoinduced behavior (both the irreversible LMCT reaction and the reversible dissociation) of these metalloporphyrins basically depends on the size (instead of the charge) of the metal center, determining the structure of

* Corresponding author. Tel.: +36 88 624159; fax: +36 88 624548.
E-mail address: otto@vegic.vein.hu (O. Horváth).

0010-8545/$ – see front matter
doi:10.1016/j.ccr.2006.02.014

these coordination compounds. Deviating from the photochemistry of the regular (coplanar) metalloporphyrins, the out-of-plane structure and the kinetic lability of the SAT complexes facilitate the photodissociation as well as the separation of the primary products of the photoinduced LMCT reaction, promoting an irreversible ring-opening of the oxidized porphyrin.

Keywords: Photochemistry; Porphyrins; Sitting-atop; Iron; Mercury; Thallium; LMCT; Photodissociation

1. Introduction

Understanding the photochemistry of metalloporphyrins has long been important in biochemistry because of their central role in photosynthesis, biological redox processes, and oxygen transport [1–10]. Despite this fact, little is known about the kinetically labile, water-soluble porphyrin complexes, especially from the viewpoint of their photoinduced properties.

Depending on their size, charge, and spin multiplicity, metal ions can fit into the central hole of the porphyrin ring, forming regular metalloporphyrins, or several of them are located out of the ligand plane, resulting in sitting-atop (SAT) complexes. The latter kind of structure induces special photophysical and photochemical features that are characteristic for all SAT complexes.

Tetrapyrrole derivatives play important roles in the nature, due to their special absorption, emission, charge transfer and complexing properties as a result of their characteristic ring structure of conjugated double bonds [11]. As to their electronic absorption, they display extreme intense bands, the so-called Soret or B bands in the 380–500-nm range, with molar extinction coefficients of $10^5\ M^{-1}\ cm^{-1}$ magnitude. Moreover, at longer wavelengths, in the 500–750-nm range, their spectra contain a set of weaker, but still considerably intense Q bands, with molar extinction coefficients of $10^4\ M^{-1}\ cm^{-1}$ magnitude. Thus, their absorption bands significantly overlap with the emission spectrum of the solar radiation reaching the biosphere, resulting in efficient tools for conversion of radiation to chemical energy. In such a conversion, the favorable emission and energy transfer properties of porphyrin derivatives are indispensable as in the case of chlorophylls, which contain magnesium ion (of 72 pm ionic radius) in the core of the macrocycle. Thus, metalloporphyrins can also be utilized in artificial photosynthetic systems, modeling the most important function of the green plants [12].

Since porphyrins generally possess considerably long-lived triplet excited states (with lifetimes in the μs–ms range), they can be very good sensitizers in photodynamic therapies [13–15]. With their energy excess, triplet excited-state porphyrins formed upon irradiation, can produce singlet oxygen molecules in the irradiated volume of the body. Thus, the locally generated singlet oxygen molecules damage the cells only in their close environment, ensuring efficient curing methods.

Due to their extensive conjugated double bond system and ring structure, porphyrins, especially their metal complexes can function as good charge transfer or electron-relay compounds. Cytochromes involving Cu^{2+} (73 pm ionic radius) or Fe^{2+} ions (75 pm (low-spin) or 92 pm (high-spin) ionic radius) in their centers are the most typical natural examples for this role in both plants and animals as well as in the human body. Similarly, in the hemo- or myoglobins in our blood, the prosthetic group containing iron(II) ion can bind and transport molecular oxygen in an axial position of the octahedral complex the equatorial sites of which are occupied by the pyrrolic nitrogens of the porphyrin ring [1,2].

Most of the natural metalloporphyrins are of regular type, i.e. their metal centers are located within the plane of the macrocyclic ligand as a consequence of their fitting size. Their ionic radii are in the range of 55–80 pm corresponding to the sphere in the porphyrin core surrounded by the four pyrrolic nitrogens. While the symmetry group of the free-base porphyrins is D_{2h} due to the two hydrogen atoms on the diagonally located pyrrolic nitrogens (Fig. 1A), the coplanar (regular) metalloporphyrins (without these protons) are of higher symmetry (D_{4h}, Fig. 1B) [16]. Deviating from the regular porphyrins, in the sitting-atop (SAT) complexes, the metal centers are located out of the ligand plane, distorting it and causing lower symmetry (C_2, Fig. 1C, but, e.g., C_{4v} "dome" or S_4 "sattle" can also occur, depending on the position of the substituents). This structure is characterized by special photophysical and photochemical features as well as offers the possibility for formation of bi- and even trinuclear (bis-porphyrin) complexes [17]. Interestingly, in the case of lanthanide ions as metal centers, triple decker porphyrin sandwich complexes were also synthesized and studied [18]. Moreover, some heavy metal ions (such as Hg^{2+}, Cd^{2+}, and Pb^{2+}) catalyze the generation of regular metalloporphyrins via formation of SAT complexes as intermediates [19] (Scheme 1).

While the natural porphyrin derivatives are exclusively hydrophobic, some artificial porphyrins having ionic substituents made it possible to prepare water-soluble metalloporphyrins of both regular and SAT type. In this work, some metal ions, each with two different oxidation states (i.e., charges), have been investigated with respect to the formation and photoinduced properties of their complexes with an anionic porphyrin (5,10,15,20-tetrakis(4-sulfonatophenyl)porphyrin, abbreviated as H_2TPPS^{4-}).

The metal ions studied from the viewpoint of formation of $TPPS^{6-}$ complexes are the following (indicating their ionic radii in brackets): Fe^{3+} (65 pm), Fe^{2+} (high-spin, 92 pm), Tl^{3+} (95 pm), Tl^{+} (147 pm), Hg^{2+} (102 pm), and Hg_2^{2+} (127 pm – for one mercury atom of the dication) [20,21]. These studies revealed how the charge and, especially the size of the metal center influence the structure and the photoinduced properties of their water-soluble porphyrin complexes. As a comparison, measurement were made with Al^{3+} (53 pm) as well, which forms typical coplanar (regular) metalloporphyrin. All the experiments the results of which are discussed in this review were carried out at room temperature and in the absence of oxygen, unless it is otherwise stated. The minimum energy

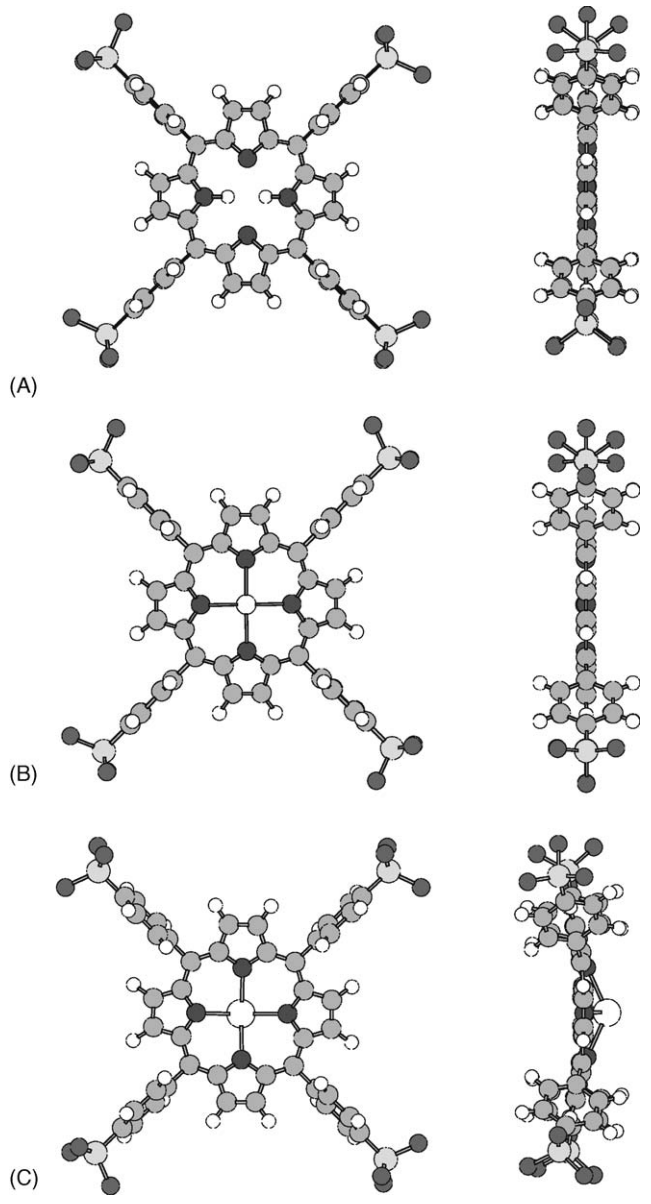

Fig. 1. Top- and side-views of a free-base porphyrin (5,10,15,20-tetrakis(4-sulfonatophenyl)porphyrin, H_2TPPS^{4-}) (A), and of its complexes with Al^{3+} (regular) (B), and Hg^{2+} (sitting-atop, SAT) (C).

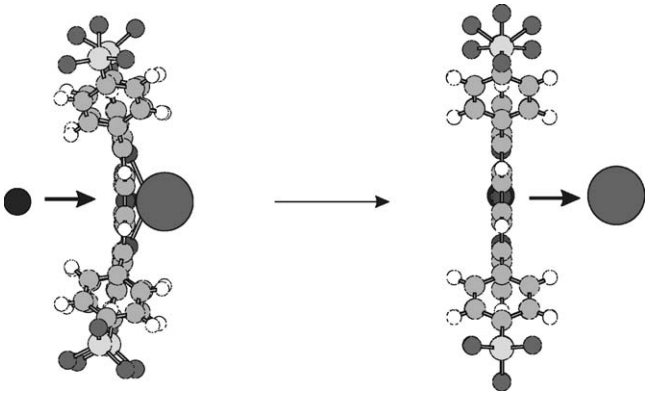

Scheme 1. Displacement of the weakly bonding metal center of an intermediate SAT complex in the synthesis of a regular metalloporphyrin.

structures reported in the present paper were obtained at the B3LYP/LANL2DZ level [22–24] using the Gaussian 98 suite of programs [25].

2. Spectral, structural and photoinduced properties of metalloporphyrins

2.1. General spectral features; molecular orbitals and spectra of metalloporphyrins

Before discussing of the properties of the individual complexes formed with the metal ions studied, it is useful to compare the general spectral features of a typical regular and a SAT metalloporphyrin together with those of the corresponding free-base porphyrin (H_2TPPS^{4-}). Fig. 2 shows the most characteristic ranges of both the absorption and the emission spectra of $HgTPPS^{4-}$, $AlTPPS^{3-}$, and H_2TPPS^{4-} (abbreviated as HgP, AlP, and H_2P). From the absorption spectra the Soret bands assigned to the $S_0 \rightarrow S_2$ transitions in the 380–440-nm range and the Q bands assigned to the $S_0 \rightarrow S_1$ are shown in the 500–700-nm range, while the emission spectra show the $S_1 \rightarrow S_0$ transitions in the 580–780-nm range. The two bands in the emission spectra are assigned to (0, 0) and (0, 1) transitions with respect to vibrational states. As the absorption

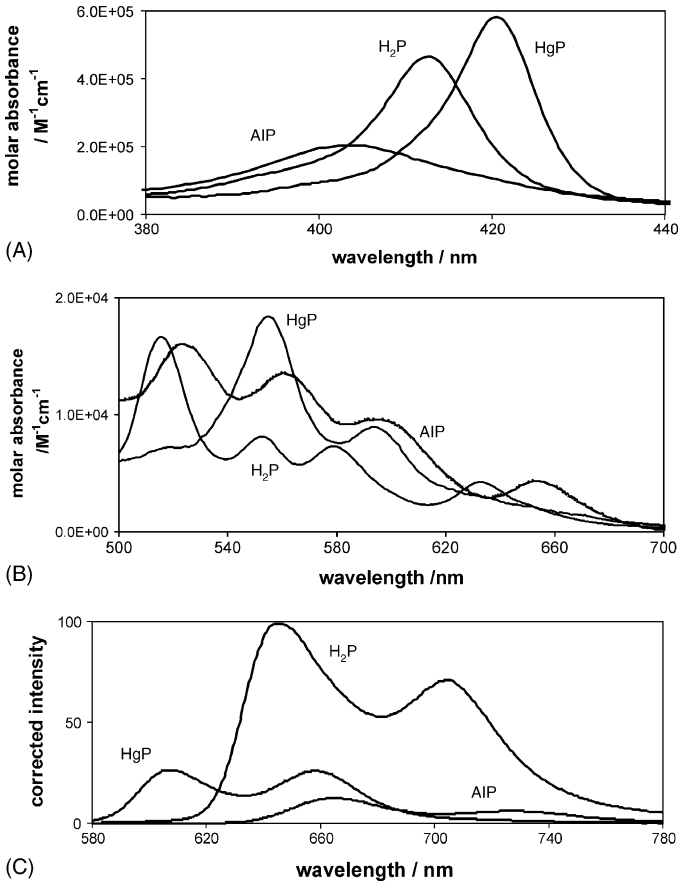

Fig. 2. Absorption spectra in the range of Soret (A) and Q (B) bands and emission spectra (C) of a free-base porphyrin (H_2TPPS^{4-} abbreviated as H_2P), and of its complexes with Al^{3+} ($Al(III)TPPS^{3-}$ abbreviated as AlP, regular) and Hg^{2+} ($Hg(II)TPPS^{4-}$ abbreviated as HgP, SAT) in aqueous solutions.

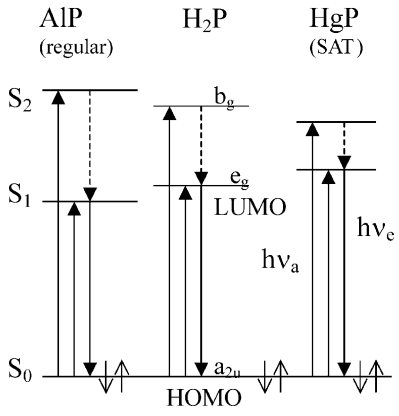

Scheme 2. Simplified energy-level diagram of the frontier orbitals of a porphyrin in free-base state (H_2P), in a regular (AlP) and in a SAT (HgP) metalloporphyrin. Abbreviations see under Fig. 2.

spectra indicate, the position of the Soret band of the typical regular metalloporphyrin Al(III)TPPS^{3-} is blue-shifted (and significantly weaker) compared to that of the free-base porphyrin. On the contrary, Hg(II)TPPS^{4-}, one of the first examples of SAT complexes, displays a red-shifted (and somewhat more intense) Soret band. The relation of the Q bands and the emission bands shows just the opposite situation, i.e., a blue shift can be seen in the case of the SAT complex (Hg(II)TPPS^{4-}) and a red shift for the regular metalloporphyrin (Al(III)TPPS^{3-}). Notably, the emission bands of both complexes are less intense than those of the free-base porphyrin. The shifts indicate that in regular metalloporphyrins the energy difference between the HOMO (a_{2u}) and the b_g MO of the ligand is larger than in the free-base porphyrin, while this difference in the SAT complex is smaller. The LUMO (e_g)–HOMO energy difference, however, is reduced in the coplanar metalloporphyrin, and increased in the SAT complex compared to H_2P (Scheme 2).

Probably due to the different overlaps between the empty atomic (s and p) orbitals of the metal center and the unoccupied b_g and e_g orbitals of the ligand (as a consequence of the significant deviation in the location of the metal ion) the changes in the energy levels of the porphyrin orbitals are markedly different, causing opposite shifts of the bands in the spectra of the regular and SAT complexes.

2.2. Iron complexes of TPPS^{6-}

2.2.1. Formation and spectra

While the radius of the Fe^{3+} ion, even in high-spin state is only 65 pm that of the high-spin Fe^{2+} ion is 92 pm. Notably, in low-spin state it is 75 pm, which in terms of size is right at the borderline between the regular and SAT complexes. Due to this strong spin-state dependence of the ionic radius of Fe^{2+} in this critical range, the structure of the heme part of the hemoglobin is dramatically affected by the coordination of O_2, changing the spin state (i.e., the size) and, thus, the location of the iron(II) as metal center [21,26]. While in deoxyhemoglobin, in high-spin state (95 pm) it is above the porphyrin plane, having an empty coordination site on the opposite side, in oxyhemoglobin, in low-spin state (75 pm) it is in the middle of the ligand core, being accessible for the oxygen molecule coordinated in axial position from below (Scheme 3). Of course, this change in the spin state and position of the metal center upon coordination of oxygen is just one of the several concerted changes in the heme part and its protein environment. Nevertheless, ab initio calculations also confirmed that iron(II) porphyrins have sitting-atop structure only in the case of a high-spin configuration of the metal center [27].

As it has been mentioned in Section 1, larger metal ions (such as Cd^{2+}, Hg^{2+} or Pb^{2+}) can catalyze the production of regular metalloporphyrins (e.g., of Zn^{2+}) via formation of SAT complexes as intermediates. The earlier experiences which indicated that iron(III) porphyrin complexes could only be synthesized by using iron(II) (instead of iron(III)) salts as reagents suggested for us the catalytic role of the Fe^{2+} ion in this process. Our recent experiments gave unambiguous evidence of this assumption. While no direct complexation takes place in aqueous solution of H_2TPPS^{4-} and Fe^{3+} even for a week, the presence of Fe^{2+} ions promotes the 100% conversion of the porphyrin to Fe(III)TPPS^{3-} within hours [28]. We think that the same way the large metal ions catalyze the formation of regular zinc(II) porphyrin via SAT complex, larger iron(II) ions also catalyze formation of the porphyrin complex of smaller iron(III) ions. The primary step of this process is the coordination of iron(II) to the one side of the porphyrin ring, forming a SAT complex. During this complexation the ligand is distorted and two new coordination positions arise on the other side of the porphyrin plane (on two diagonally situated nitrogen atoms) and become more accessible for the iron(III) ions (Scheme 4). The subsequent coordination of iron(III) is followed by the detachment of the more weakly bounded iron(II) ion, and, at the end of the substitution, Fe^{3+} occupies the very center of the ligand. The Fe(III)TPPS^{3-} complex formed is a kinetically inert (non-SAT) regular metalloporphyrin, i.e., this substitution is irreversible. An alternative mechanism could be an inner- or outer-sphere electron transfer between the complexed iron(II) center and a iron(III) ion approaching from the bulk. However, we think this mechanism less favorable because the iron(II) porphyrin complex was found to be not sensitive to the presence of oxygen (see below).

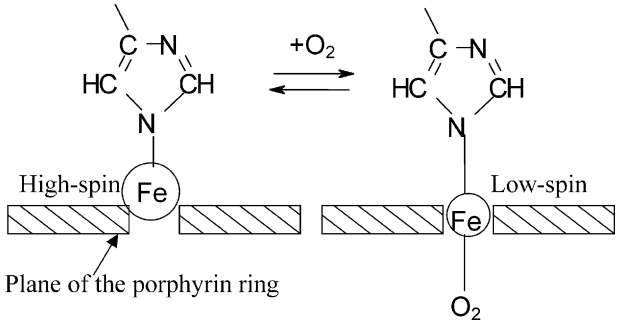

Scheme 3. The change of the spin state, i.e., the size of the iron(II) center in the hemoglobin upon coordination of oxygen.

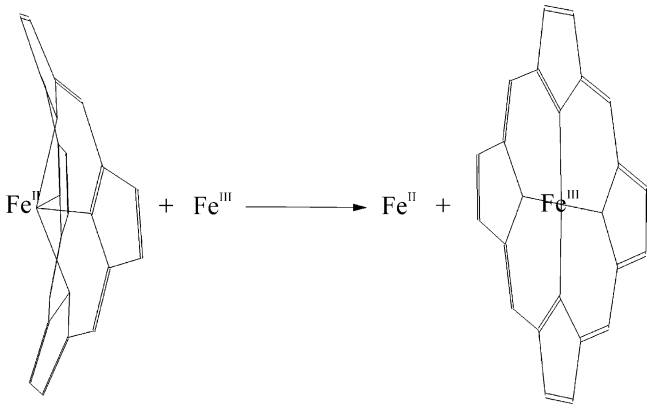

Scheme 4. Displacement of iron(II) (as catalyst) from an intermediate SAT complex in the synthesis of iron(III) porphyrin. (Adapted from Ref. [28].)

On the basis of our observations, iron(II) porphyrin complex can only be prepared in the total absence (even trace amounts) of iron(III). This was achievable in argon-saturated solution (containing iron powder) by application of acetate buffer, which is a good trap for iron(III), and which stabilizes the pH above 5.5 to avoid the protonation of the free-base porphyrin [28]. It is noteworthy that addition of oxygen to this system, after the generation of Fe(II)TPPS^{4-}, does not lead to the conversion of the iron(II) porphyrin to iron(III) porphyrin. Although dissolved oxygen oxidizes uncomplexed Fe^{2+} ions (but not the complexed ones), the Fe^{3+} ions formed are trapped by acetate, hindering their reaction with the iron(II) porphyrin complexes.

The absorption and emission spectra of the iron TPPS^{6-} complexes (compared to those of the free-base porphyrin, Fig. 3) clearly indicate that Fe(III)TPPS^{3-} is a typical regular metalloporphyrin with blue-shifted Soret band (and Q bands as well). It does not show any fluorescence, which is not surprising for a paramagnetic regular metalloporphyrin. The absorption spectrum of Fe(II)TPPS^{4-}, however, displays red-shifted bands characteristic for the SAT complexes, which is in accordance with the blue-shifted emission bands. These properties suggest that the size of the metal center (with the same metal but with different charges) markedly influences the structure of the metalloporphyrin, and, thus, its spectral features. Photochemical behavior of these complexes provides further evidence for this conclusion.

2.2.2. *Photoredox chemistry*

Photolysis of Fe(II)TPPS^{4-} at both the Soret and the Q bands leads to the degradation of the complex itself, indicated by the disappearance of the Soret and Q bands, accompanied by the formation of ring-opened tetrapyrrole derivatives (bile type pigments) indicated by the new, arising bands (Fig. 4) [28]. The first step of this photoinduced process is an electron transfer from the porphyrin ligand to the metal center (LMCT), followed by an irreversible ring-opening and the reoxidation of the detached iron(I) species.

In the case of Fe(III)TPPS^{3-}, a regular metalloporphyrin, irradiation under the same conditions causes no permanent chemical change. In blank experiments with the free-base porphyrin in the absence of metal centers, the quantum efficiency of its photoinduced degradation was found to be negligible (6.0×10^{-6} in air-saturated and 3.4×10^{-6} in deoxygenated solution) at Soret-band irradiation, and no permanent change was observed upon Q-band excitation. This clearly indicates that the coordination of relatively large metal ions to the porphyrin results in new, more efficient photoredox activity of the SAT complexes formed compared to that of the free-base porphyrin.

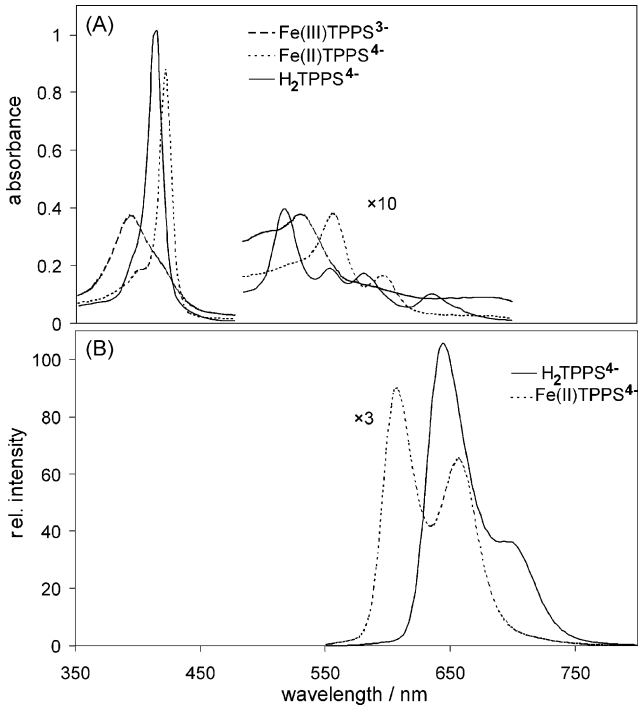

Fig. 3. Ground-state absorption and emission spectra of H_2TPPS^{4-}, Fe(II)TPPS^{4-} and Fe(III)TPPS^{3-} in water (λ_{exc} = 421 nm). (Adapted from Ref. [28].)

While additional axial ligands are well known to participate in photoredox processes (e.g., in the case of iron(III) complexes), a light-induced electron exchange between a metal and its porphyrin ligand is rather unusual for regular metalloporphyrins. If it should occur as primary photochemical step, an efficient back electron transfer takes apparently place since permanent redox products are not observed. In the case of a SAT complex such as

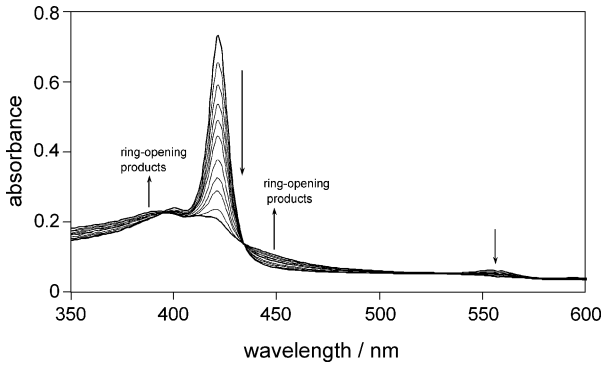

Fig. 4. Degradation of Fe(II)TPPS^{4-} and formation of ring-opening products upon irradiation at 421 nm. (Adapted from Ref. [28].)

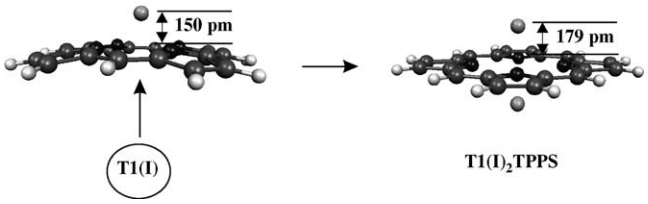

Scheme 5. Structural change during the formation of $Tl(I)_2TPPS^{4-}$. (The sulfonatophenyl groups are omitted for the sake of simplicity.)

that of iron(II), the out-of-plane structure and the kinetic lability seem to facilitate a separation of the redox products.

2.3. Thallium complexes of $TPPS^{6-}$

2.3.1. Formation and spectra

In contrast to the case of iron, where both Fe^{2+} and Fe^{3+} form 1:1 complex with $TPPS^{6-}$, the composition of the metalloporphyrins containing thallium ion strongly depends on the oxidation state of the metal center. While Tl^{3+} of 95 pm ionic radius forms 1:1 complex with porphyrins [29–31], Tl^+ ions, due to their relatively huge size ($r = 147$ pm), coordinate to the porphyrin ligand on both side of its plane as can be seen in Scheme 5 displaying the molecular structures determined by DFT calculations. The calculated distance between the metal centers in $Tl(I)_2TPPS^{4-}$ (358 pm) agrees well with that determined by X-ray diffraction for a similar bis-thallium(I) porphyrin complex (330 pm) [32]. Interestingly, no complex of 1:1 composition has been detected so far, not even in a preparation process using 1:1 ratio of the Tl^+ and porphyrin reagents. Instead, besides the formation of a 2:1 complex, one half of the porphyrin was left unreacted [32]. This phenomenon can be interpreted by the extremely large difference between the sizes of the two thallium ions. In the case of iron, formation of 1:1 complexes is possible for both Fe^{2+} (radius 92 pm) and Fe^{3+} (radius 65 pm) because both ions are small enough to be immersed, at least partially, into the porphyrin core. In the case of thallium, the charge difference is 2 between Tl^+ and Tl^{3+}, so that their ion size differs so much that the behavior of the two oxidation states is qualitatively different. While the thallium(III) ion (radius 95 pm) is small enough to fit (at least partly) into the core of the porphyrin ligand (like iron(II) of 92 pm radius), the large thallium(I) ion (radius 147 pm) cannot fit (even partly), and is located completely out of the ligand plane. Analogous behavior of Ag^+ ions (of similarly large ionic radius, 126 pm), i.e., formation of 2:1 complexes was observed with cationic porphyrins [33]. The lack

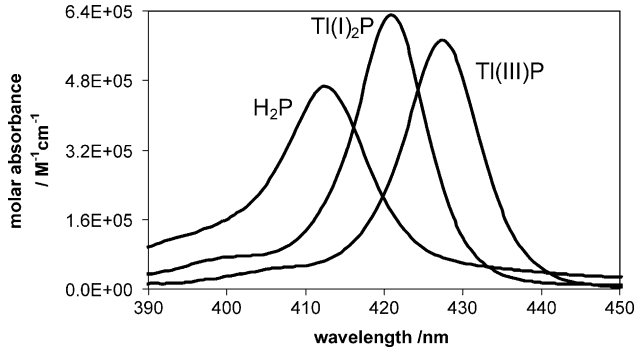

Fig. 5. Soret bands of the free-base porphyrin, H_2TPPS^{4-} (H_2P) and of its complexes with Tl^+ ($Tl(I)_2TPPS^{4-}$, abbreviated as Tl(I)2P) and Tl^{3+} ($Tl(III)TPPS^{3-}$, abbreviated as Tl(III)P). (Adapted from Refs. [35,36].)

of detection of the 1:1 complex (at least in the 1–100 s time range) indicates that the binding of the first metal ion distorts the porphyrin ring, and, thus promotes the coordination of the second one (as demonstrated in Scheme 5). This behavior is in accordance with the catalytic effect of larger metal ions in the preparation of regular metalloporphyrins [19,34]. Deformation of the porphyrin ligand due to the coordination of the catalyst ion to one side facilitates the entrance of the other metal ion (of smaller radius) from the opposite side. The rather weak interaction between the ligand and the thallium(I) ions of large diameter and small charge is also demonstrated by the rather low complex formation constant compared to that of $Tl(III)TPPS^{3-}$, where the much smaller thallium(III) ion with +3 charge is considerably more strongly bound to the porphyrin (Table 1) [35,36].

Despite the difference in the composition, structure, and stability of the Tl^+ and Tl^{3+} porphyrin complexes, their spectral features are rather similar. Compared to the absorption bands of the free-base porphyrin, red shifts of the corresponding bands of both thallium porphyrins are observed in the ranges of the Soret bands (Fig. 5).

Such a behavior suggests that these complexes are of SAT type. Notably, the band shifts in the case of $Tl(I)_2TPPS^{4-}$ are significantly smaller (about half) than those for $Tl(III)TPPS^{3-}$, due to the considerably weaker metal–ligand interaction. Nevertheless, the positions of the corresponding fluorescence bands are almost the same for these complexes, displaying strong blue shifts compared to the case of free-base porphyrin, confirming the SAT features of these metalloporphyrins (Fig. 6). The stronger interaction (partly heavy-atom effect) in the case of Tl^{3+} is manifested in the much lower intensity of the emission

Table 1
Formation constants, characteristic absorption and emission data of $Tl(I)_2TPPS^{4-}$ and $T(III)TPPS^{3-}$, compared to those of the free-base porphyrin (H_2TPPS^{4-})

	$Tl(I)_2TPPS^{4-}$	$Tl(III)TPPS^{3-}$	H_2TPPS^{4-}
Ionic radius of the metal center/pm	147	95	–
Formation constant, lg (β/[H^+])	3.55	6.98	–
Soret band, λ_{max}/nm (ε_{max}/M^{-1} cm^{-1})	421 (631000)	428 (573000)	413 (466000)
Q bands, λ_{max}/nm (ε_{max}/M^{-1} cm^{-1})	555 (22810), 594 (9830)	562 (21130), 603 (10850)	516 (16700), 553 (8150), 579 (7290), 633 (4250)
Fluorescence, λ_{max}/nm	610, 659	611, 663	647, 703
Φ_{fl}	0.0131	0.00022	0.056
Reference	[35]	[36]	[35,37]

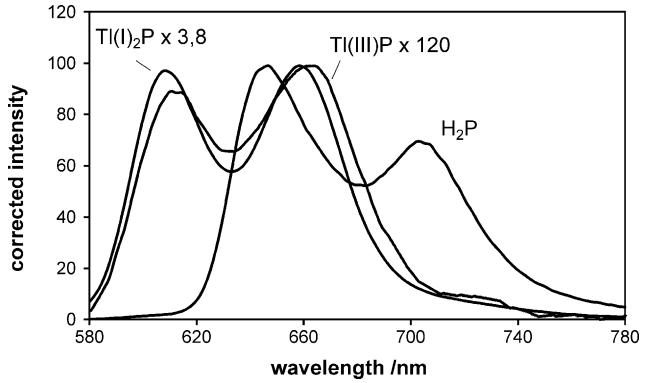

Fig. 6. Fluorescence spectra of the free-base porphyrin, H_2TPPS^{4-} (H_2P) and of its complexes with Tl^+ ($Tl(I)_2TPPS^{4-}$, abbreviated as $Tl(I)_2P$) and Tl^{3+} ($Tl(III)TPPS^{3-}$, abbreviated as Tl(III)P). The coefficients indicate the amplification applied for the sake of approximately equal intensity. (Adapted from Refs. [35,36].)

bands, i.e. much less efficient $S_1 \rightarrow S_0$ radiative transitions. This is also shown in Table 1.

2.3.2. Photoredox chemistry

Similarly to the case of $Fe(II)TPPS^{4-}$, irradiation of both $Tl(III)TPPS^{3-}$ and $Tl(I)_2TPPS^{4-}$ resulted in irreversible degradation of the complexes. The primary step in this process, which is typical for SAT metalloporphyrins, is a ligand-to-metal charge transfer producing oxidized porphyrin and reduced metal center. Since the stability of $Tl(III)TPPS^{3-}$ is rather high, it can be studied in solution containing Tl(III) and porphyrin in equimolar concentrations. Irradiation of such a solution leads to the destruction of the complex, accompanied by the simultaneous appearance of the free-base porphyrin as demonstrated in Fig. 7 [36]. This phenomenon indicates that irreversible oxidation of one porphyrin ligand results in the reduction of two Tl^{3+} ions to Tl^+, i.e. the overall change of the oxidation number is 4. This result is in accordance with the behavior of $Hg(II)TPPS^{4-}$ [39] as discussed later. Irradiation at both the Soret and the Q bands leads to irreversible photooxidation of the porphyrin ligand in these complexes. In larger metal center a higher quantum yield can be expected for this photoinduced reaction because of the enhancement of the detachment of the reduced metal from the ligand. Accordingly, the quantum efficiencies for the degradation of $Tl(I)_2TPPS^{4-}$ are at least one order of magnitude higher

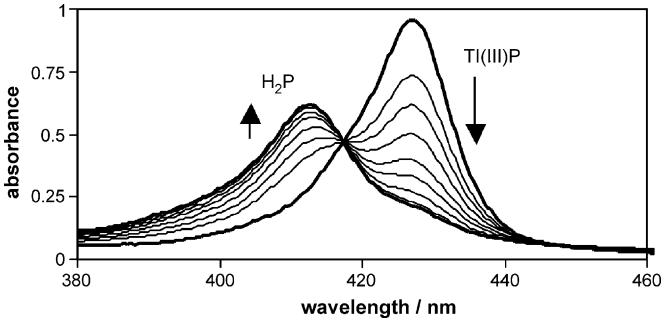

Fig. 7. Spectral change during the photolysis of aqueous solution containing 3×10^{-6} M thallium(III) and porphyrin, each ($\lambda_{irr} = 428$ nm). Abbreviations: H_2P is H_2TPPS^{4-} and Tl(III)P is $Tl(III)TPPS^{3-}$. (Adapted from Ref. [36].)

Table 2
Characteristic quantum yields ($\Phi \times 10^4$) for the photoinduced degradation of $Tl(I)_2TPPS^{4-}$ and $Tl(III)TPPS^{3-}$, compared to those of the free-base porphyrin (H_2TPPS^{4-})

Conditions	$Tl(I)_2TPPS^{4-}$	$Tl(III)TPPS^{3-}$	H_2TPPS^{4-}
Soret-band irradiation			
Deoxygenated	3.5	0.145	0.034
Aerated	3.4	0.28	0.063
Q-band irradiation			
Deoxygenated	2.9	0.26	–
Aerated	2.9	0.149	–
Reference	[35], this work	[36]	[35]

than those for the reaction of the thallium(III) porphyrin at both Soret- and Q-band irradiations (Table 2) [35,36].

The final products of this photoinduced process are bilirubin- and biliverdin-type derivatives due to the ring-opening following the detachment of the reduced metal center. As the quantum yield data of Table 2 shows the reaction is not really oxygen sensitive. Moreover, it has also been shown experimentally that the role of charge transfer to solvent (CTTS) reaction, i.e., direct photoelectron ejection from the porphyrin ligand is not significant, not even at Soret-band excitation [35].

2.4. Mercury complexes of $TPPS^{6-}$

2.4.1. Hg^{2+} complexes of $TPPS^{6-}$

2.4.1.1. Formation, spectra, and structures. The study of the Hg^{2+} complexes of $TPPS^{6-}$ began more than 20 years ago. Adeyemo and Krishnamurthy [38] found unambiguous spectral evidence for the formation of 1:1 complex, which was confirmed by recent experiments [39]. However, regarding the composition of complexes formed at higher ligand and mercury(II) concentrations, varying results and conclusions were published, suggesting the appearance of 2:1 [40,37] or 3:2 [38] complexes. Quite recent investigations based on thorough evaluation of photometric titration data presented strong evidences for the formation of the 3:2, and, what has never been even suggested before, the 2:2 complexes [41]. As Fig. 8 shows, the Soret bands of all three of these complexes are red-shifted compared to that of the free-base porphyrin, suggesting they are SAT type. Interestingly, the

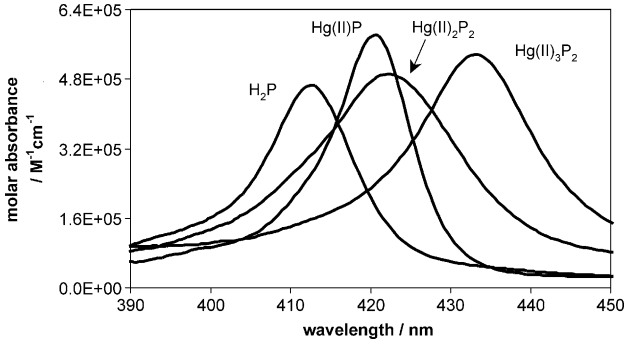

Fig. 8. Soret bands of the free-base porphyrin H_2TPPS^{4-} (H_2P) and of its various complexes with Hg^{2+}. Abbreviations: Hg(II)P is $Hg(II)TPPS^{4-}$, $Hg(II)_2P_2$ is $Hg(II)_2(TPPS)_2^{8-}$, and $Hg(II)_3P_2$ is $Hg(II)_3(TPPS)_2^{6-}$. (Adapted from Refs. [39,41].)

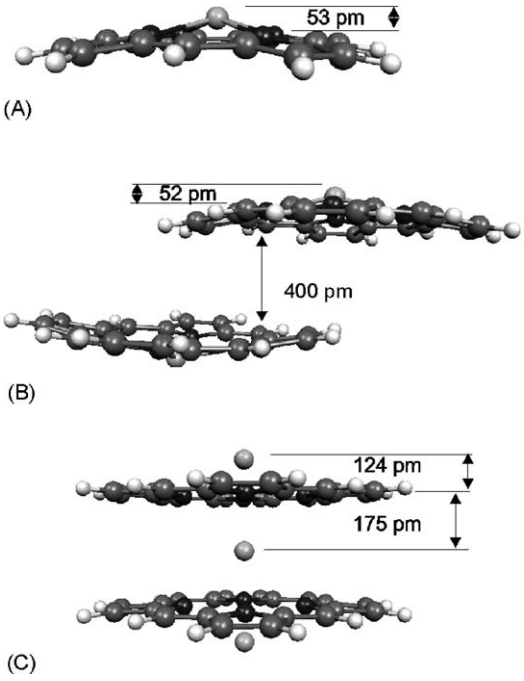

Fig. 9. Structures of $Hg(II)TPPS^{4-}$ (A), $Hg(II)_2(TPPS)_2^{8-}$ (B), and $Hg(II)_3(TPPS)_2^{6-}$ (C) determined by DFT calculation. (Adapted from Ref. [41].)

Soret band of the dimer, i.e., the 2:2 complex, is only slightly (about 85 cm^{-1}) red-shifted compared to the monomer (1:1 complex), although it is significantly broadened, and its maximum molar absorbance is somewhat lower. The Soret band of the 3:2 complex is much more (about 685 cm^{-1}) red-shifted with a somewhat "sharper" peak. This tendency unambiguously shows that increasing the number of the porphyrin ligands and, especially, of the metal centers, causes stronger red shift of the Soret band, and the Q bands as well, as Table 3 indicates. Surprisingly, only the 1:1 complex displays fluorescence at room temperature. In the case of excited-state bis-porphyrin derivatives other relaxation pathways are favored. DFT calculations [41] confirmed that the structure of the 1:1 complex is of typically sitting-atop, where the center of the coordinated mercury(II) ion is about 53 pm above the plane of the pyrrole nitrogens (Fig. 9).

This calculated distance between the metal center and the ligand plane is in very good agreement with the value (56 pm) determined by X-ray diffraction for a similar 1:1 mercury(II) porphyrin complex [42].

In the dimer, the corresponding distance is almost the same (52 pm), where the core of the porphyrin rings are shifted toward each others, and the distance between their mean planes is about 400 pm. No appreciable shift in the positions of the ligands occurs in the case of the 3:2 complex, where the distances between the mercury(II) ions and the porphyrin planes are much larger due to the strong repulsion and steric effect. The outer mercury(II) ions are located 124 pm from the mean planes of porphyrin rings, while the third metal center (in the middle) is 175 pm from the ligands [41]. Thus, the distance between the central and the outer metal ions is about 300 pm, which is consistent with the value of 310 pm determined earlier for the Hg–Hg distance by EXAFS measurements in the Hg^{2+}-$TPPS^{6-}$ system at higher concentrations [37]. In the 3:2 complex the porphyrin planes are closer (350 pm) to each other than in the case of the dimer, indicating a stronger interaction via the middle mercury(II) ion. Probably this stronger connection and, thus, the shorter ligand–ligand distance causes the 45° rotation of the one porphyrin ring to the other as shown by the DFT calculations. These data are in good agreement with the orders of magnitude of the equilibrium constants for the following stepwise formation reactions [39,41]:

$$Hg^{2+} + H_2TPPS^{4-} \Leftrightarrow Hg(II)TPPS^{4-} + 2H^+$$
$$K_{1'} = K_1/[H^+]^2 = 8.8 \times 10^5\ M^{-1} \quad (1)$$

$$2Hg(II)TPPS^{4-} \Leftrightarrow Hg(II)_2(TPPS)_2^{8-}$$
$$K_{2:2} = 7.2 \times 10^2\ M^{-1} \quad (2)$$

$$Hg(II)_2(TPPS)_2^{8-} + Hg^{2+} \Leftrightarrow Hg(II)_3(TPPS)_2^{6-}$$
$$K_{3:2} = 6.2 \times 10^3\ M^{-1} \quad (3)$$

The insertion of the third mercury(II) center in between the porphyrin planes results in a higher thermodynamic stability for the bis-porphyrin complex.

2.4.1.2. Photoinduced reactions. Hg^{2+}-$TPPS^{6-}$ complexes represent the first examples for the unique photochemical behavior of the SAT metalloporphyrins [39]. Similarly to the $TPPS^{6-}$ complexes of thallium and iron(II), complexes of thallium and iron(II), irradiation of the Hg^{2+}-$TPPS^{6-}$ complexes leads to an irreversible redox degradation as shown by the disappearance of the characteristic Soret band in the absorption spectrum of $Hg(II)TPPS^{4-}$ (Fig. 10). This process is accompanied by

Table 3
Characteristic absorption and emission data of mercury(II) complexes of $TPPS^{6-}$

	$Hg(II)TPPS^{4-}$	$Hg(II)_2(TPPS)_2^{8-}$	$Hg(II)_3(TPPS)_2^{6-}$
Soret band, λ_{max}/nm (ε_{max}/M^{-1} cm^{-1})	421 (583000)	422 (491000)	433 (533000)
Q bands, λ_{max}/nm (ε_{max}/M^{-1} cm^{-1})	555 (18400), 594 (8950)	580 (16700), 628 (15500)	590 (16300), 628 (16000)
Fluorescence, λ_{max}/nm	606	–	–
Φ_{fl}	0.016	–	–
Reference	[39]	[41]	[41]

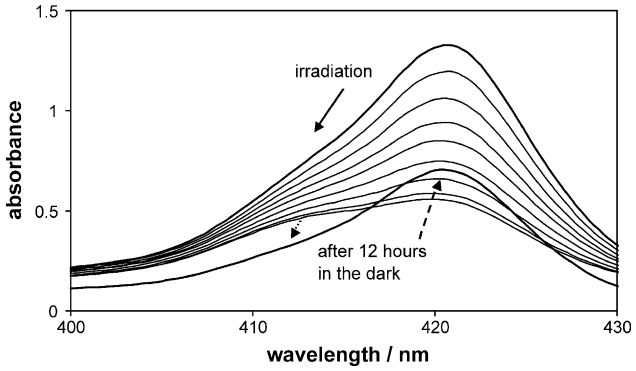

Fig. 10. Spectral change during the photolysis (λ_{irr} = 421 nm) of aqueous solution containing 5.3×10^{-7} M porphyrin and 4.5×10^{-6} M mercury(II) at pH 7. Under these conditions, Hg(II)TPPS^{4-} is the only metalloporphyrin species in the system. (Adapted from Ref. [39].)

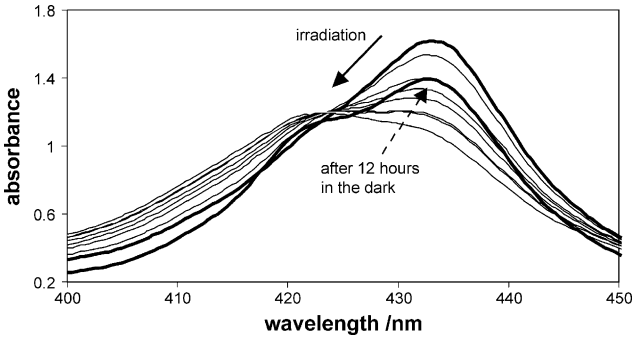

Fig. 11. Spectral change during the photolysis (λ_{irr} = 433 nm) of aqueous solution containing 6.9×10^{-6} M porphyrin and 1.5×10^{-3} M mercury(II) at pH 7. Under these conditions, Hg(II)$_3$(TPPS)$_2^{6-}$ is the predominant metalloporphyrin species in the system, its partial molar fraction is 0.9. (Adapted from Ref. [41].)

the formation of free-base porphyrin indicated by the appearance of a shoulder at 413 nm. The latter phenomenon suggests a dissociation of the complex simultaneously occurring with the irreversible redox reaction. This dissociation proved to be reversible, as indicated by the partial regeneration of the disappeared Hg(II)TPPS^{4-} complex along with the re-coordination of the released free-base porphyrin after keeping the photolyzed solution in the dark for 12 h (Fig. 10). At Soret-band excitation in argon-saturated solution, the quantum yields for the simultaneous redox degradation and dissociation are 2.1×10^{-4} and 1.6×10^{-5}, respectively [39]. Irradiation of the Hg(II)TPPS^{4-} complex at the Q bands (λ_{ir} = 555 nm) also leads to the degradation of this metalloporphyrin ($\Phi_{redox} = 3.3 \times 10^{-4}$), but, interestingly, no dissociation can be observed in this case [39]. These results indicate that dissociation occurs from singlet excited state, and the extra energy at the Soret-band excitation promotes this reaction and other energy-dissipating processes, diminishing the efficiency of the redox reaction.

Soret-band irradiation of the 2:2 complex leads also to redox degradation, but with lower quantum yield (1.03×10^{-4}), and to dissociation as well, with comparable efficiency (6.3×10^{-5}) [41]. These values indicate that the stability of the dimer (compared to dissociation to monomers) is lower than that of the monomer (compared to dissociation to free-base porphyrin and the metal center). Interestingly, Q-band irradiation of Hg(II)$_2$(TPPS)$_2^{8-}$ leads also to both redox reaction and dissociation, with the quantum yields of 2.8×10^{-5} and 2.1×10^{-5}, respectively. These values suggest that lower-energy excitation too is enough for the dissociation of the 2:2 complex, but the efficiency of the redox degradation significantly drops in this case [41].

Similarly to Hg(II)TPPS^{4-} and Hg(II)$_2$(TPPS)$_2^{8-}$, the 3:2 complex also undergoes both irreversible redox degradation and reversible dissociation upon Soret-band irradiation (Fig. 11). Dissociation reaction in this case leads to the formation of free-base porphyrins too as indicated by the temporary absorption increase at 411 nm. The quantum yields for these reactions of Hg(II)$_3$(TPPS)$_2^{6-}$, however, are about two orders of magnitude higher than those for the cases of Hg(II)TPPS^{4-} and Hg(II)$_2$(TPPS)$_2^{8-}$. Besides, the efficiency of the redox degradation (6.8×10^{-3}) is significantly lower than that of the dissociation (2.3×10^{-2}) [41]. These results are in very good agreement with the structural data determined by DFT calculations (see Fig. 9). Because of the much larger distances between the porphyrin planes and the mercury(II) centers in the 3:2 complex compared to those in the Hg(II)TPPS^{4-} and Hg(II)$_2$(TPPS)$_2^{8-}$ species (124/175 pm versus 52–53 pm), the coordination bond in the previous case is much weaker promoting a much easier dissociation upon excitation. Moreover, the detachment of the reduced metal center after a photoinduced LMCT step is much more favorable in this case. Although the quantum yield for the redox reaction upon Q-band irradiation is rather low (2.1×10^{-5}), the efficiency of the dissociation is two orders of magnitude higher (2.0×10^{-3}). This behavior is the reverse of that observed at the Hg(II)TPPS^{4-} species, due to the strong structural deviations. Degradation of the Hg^{2+}-TPPS^{6-} complexes is accompanied by the formation of Hg_2^{2+}, the concentration of which can be determined by measuring its absorbance at 237 nm (due to the $\sigma \rightarrow \sigma^*$ transition) [43]. On the basis of this measurement, the change in the oxidation state of the porphyrin is 4 as described by the following equation regarding Hg(II)TPPS^{4-}:

$$\text{Hg(II)TPPS}^{4-} + h\nu \xrightarrow{\text{Hg}^{2+}} 2\text{Hg}_2^{2+} + \text{products} \quad (4)$$

This result agrees perfectly with that observed in the case of the Tl(III)TPPS^{3-} complex, indicating that the metal center does not influence the measure of the redox change of the porphyrin ligand.

2.4.2. Hg_2^{2+} complexes of TPPS^{6-}

2.4.2.1. Formation, spectra, and structures. While studies of Hg^{2+}-TPPS^{6-} complexes started more than 20 years ago, investigation of the coordination compounds formed between TPPS^{6-} and Hg_2^{2+} ions has only recently begun [44]. Hg_2^{2+} represents the simplest cluster, in which the two mercury ions are connected by a σ bond. The ionic radius of the mercury(I) units (127 pm) is much larger than that of the Hg^{2+} ion (102 pm). Probably also for this reason, the composition of the most simple Hg_2^{2+}-TPPS^{6-} species, in contrast to Hg(II)TPPS^{4-}, is not 1:1. Instead, according to the results of spectrophotometric titration, at rather low porphyrin concentration (2×10^{-7} M),

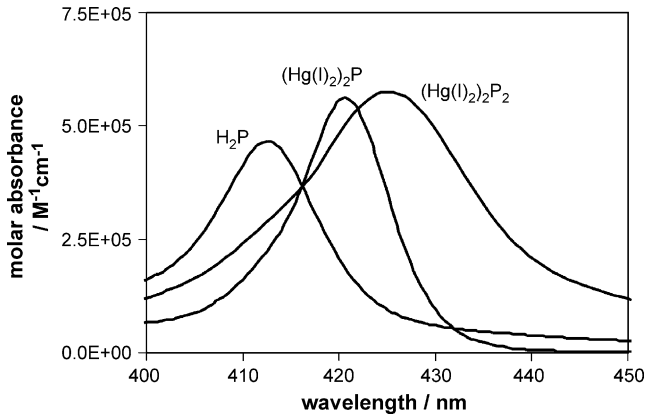

Fig. 12. Soret bands of the free-base porphyrin, H_2TPPS (H_2P) and of its complexes with Hg_2^{2+}. Abbreviations: $(Hg(I)_2)_2$P is $(Hg(I)_2)_2TPPS^{2-}$ and $(Hg(I)_2)_2P_2$ is $(Hg(I)_2)_2(TPPS)_2^{8-}$. (Adapted from Ref. [43].)

formation of 2:1 complex can be observed. Similarly to the case of thallium(I), no complex of 1:1 composition could be detected. Inspite of the structural similarity, the stability of $(Hg(I)_2)_2TPPS^{2-}$ is several orders of magnitude larger than that of $Tl(I)_2TPPS^{4-}$ ($\beta_2/[H^+]^2 = 1.15 \times 10^{10}\,M^{-2}$ versus $3.55 \times 10^3\,M^{-2}$). A possible explanation for this is the extremely large ionic radius of thallium(I) (147 pm), resulting in a rather weak coordination bond to the porphyrin. Although the composition of $(Hg(I)_2)_2TPPS^{2-}$ deviates from that of $Hg(II)TPPS^{4-}$, their absorption spectra are quite similar, and the Soret bands of both complexes are at about 421 nm (just as in the case of $Tl(I)_2TPPS^{4-}$) as shown in Fig. 12. Also the 2:1 porphyrin complex of Hg_2^{2+} displays emission with characteristic bands at 609 and 661 nm. The positions of these bands agree well with those displayed by the monoporphyrin complexes of Fe^{2+}, Tl^+, Tl^{3+}, and Hg^{2+}, indicating a typical common SAT feature. According to the DFT calculations, the distance between the porphyrin plane and closer mercury(I) units is 150 pm, due to the repulsion of the metal centers. Notably, the corresponding distance in the hypothetical 1:1 complex would only be 64 pm.

At higher porphyrin concentration (2.5×10^{-6} M), formation of 2:2 complex can be observed, the Soret band of which is displayed at 425 nm (Fig. 12) [44]. DFT calculations indicate that, deviating from the corresponding 2:2 complex of Hg^{2+}, the structure of the $(Hg(I)_2)_2(TPPS)_2^{8-}$ species is asymmetric as shown in Fig. 13. The average distance between the porphyrin planes and the closer mercury(I) units is about 74 pm in this case because the repulsion of the metal centers is almost negligible. However, the distance between the middle mercury(I) unit and the other porphyrin plane is quite large (340 pm), but comparable with the bond distance within the Hg_2^{2+} cluster (ca. 320 nm). Even so, the interaction between the connected monomers is strong enough to hinder the fluorescence of this species, similarly to the bis-porphyrin complexes of Hg^{2+}.

2.4.2.2. Photoinduced reactions. Just as in the case of the Hg^{2+}-$TPPS^{6-}$ complexes, Soret-band irradiation of $(Hg(I)_2)_2TPPS^{2-}$ in argon-saturated solution leads to both irreversible redox degradation and reversible dissociation to Hg_2^{2+} ions and free-base porphyrin. The quantum yield for the redox process ($\Phi_{redox} = 1.44 \times 10^{-4}$) is several times higher than that for the dissociation ($\Phi_{diss} = 3.1 \times 10^{-5}$). This tendency is even stronger in the case of the Q-band irradiation, where no dissociation can be observed, the only photoinduced reaction is redox degradation, with a quantum yield of 7.2×10^{-5} [44].

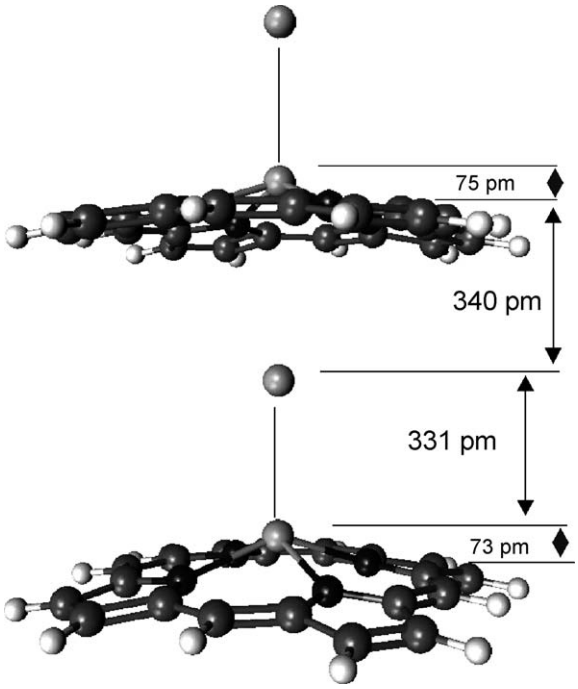

Fig. 13. Structure of $(Hg(I)_2)_2(TPPS)_2^{8-}$ determined by DFT calculations. (Adapted from Ref. [44].)

The 2:2 complex displays similar photochemical behavior. Both redox reaction with ring-opening and dissociation take place upon Soret-band irradiation. In this case, the partial molar fraction of $(Hg(I)_2)_2TPPS^{2-}$ increases during the photolysis, not only as a consequence of the dissociation, but also due to the decreasing concentration of the porphyrin. This is manifested in the gradual blue shift of the Soret band. Similarly to the 2:1 complex, the efficiency for the redox reaction ($\Phi_{redox} = 8.7 \times 10^{-5}$) is significantly higher than that for the dissociation ($\Phi_{diss} = 1.44 \times 10^{-5}$). Q-band excitation, as in the case of the bis-porphyrin complexes of Hg^{2+}, leads also to dissociation, deviating from the photochemical behavior of the monoporphyrin complexes. Moreover, the quantum yield of this process is several times higher than that of the redox degradation, although both are rather low ($\Phi_{redox} = 3.1 \times 10^{-5}$, $\Phi_{diss} = 9.0 \times 10^{-5}$). This phenomenon suggests that the redox reaction in this system requires more energy than dissociation, probably due to the relatively short out-of-plane distance of the closer mercury(I) units compared to the case of the monoporphyrin complex (74 pm versus 150 pm).

3. Summary and conclusions

In this study, the water-soluble $TPPS^{6-}$ complexes of some metal ions, each with two different oxidation states, have been investigated, in order to reveal how the charge and, especially

the size of the metal center influence their composition, structure and photoinduced properties.

One of the best examples for such a comparison is the case of the Fe^{2+} and Fe^{3+} metal centers. While the heme-like (1:1) iron(II) complex displays typical SAT behavior (red-shifted Soret absorption and blue-shifted emission and Q absorption bands, irreversible photoinduced porphyrin ligand-to-metal charge transfer reaction), the corresponding iron(III) porphyrin is a regular one with no emission and photoredox properties. Moreover, the formation of the latter complex is promoted by the kinetically labile iron(II) porphyrin (i.e., Fe^{2+} ions act as catalyst in this process).

In contrast to iron, in the case of thallium (Tl^{3+}, Tl^{+}) and mercury (Hg^{2+}, $Hg_2{}^{2+}$), all porphyrin complexes are of SAT type, regardless of the oxidation state of the metal center. Among these metalloporphyrins, however, compositions other than 1:1 occur, in accordance with the considerable diversity in the efficiencies of the emission and photoredox activities.

While thallium(III) forms 1:1 $TPPS^{6-}$ complex, the composition of the corresponding thallium(I) species is 2:1, although both the absorption and the emission spectra of these compounds are very similar. However, the quantum yields for their photoredox degradation are quite different; the efficiency is much larger in the case of the thallium(I) complex, due to its much lower stability. This is a consequence of the larger metal–porphyrin distance, i.e. the extremely large ionic radius of Tl^{+}. This example, along with the observation of Fe(II)$TPPS^{4-}$ and Fe(III)$TPPS^{3-}$ complexes, clearly indicates that the photoredox (LMCT) behavior of these metalloporphyrins basically depends on the size (instead of the charge) of the metal center, determining the structure of these coordination compounds. Otherwise, higher efficiencies would be observed for the photoredox reactions of the complexes with metal center of higher oxidation state, which is not the case.

Both Hg^{2+} and $Hg_2{}^{2+}$ also form bis-porphyrin complexes. These compounds, in contrast with from the corresponding monoporphyrin species, do not show any fluorescence at room temperature. However, the energy of the Q-band excitation is enough to promote their photoinduced dissociation, which can only be observed upon Soret-band irradiation in the case of the monoporphyrin complexes. This phenomenon is also a consequence of the structural differences.

All these results demonstrate well how strongly the size of the metal center influences the composition, the structure, and thus, the photoinduced behavior of the water-soluble metalloporphyrins, especially the sitting-atop complexes, where the measure of the out-of-plane location of the metal ion can vary in a relatively wide range. The photochemistry of SAT complexes is dominated by porphyrin ligand-to-metal charge transfer reaction and photodissociation, which are unusual for regular (coplanar) metalloporphyrins. If LMCT reaction should occur as the primary photochemical step, an efficient back electron transfer would take place in coplanar complexes since permanent redox products are not observed. In the case of SAT complexes, however, the out-of-plane structure and the kinetic lability seem to promote the photodissociation and the separation of the primary products of the LMCT step, which is followed by an irreversible ring-opening of the oxidized porphyrin. Larger metal centers (even with lower positive charge) result in more efficient photodegradation due to the more labile structure of the porphyrin complex.

Acknowledgments

Many thanks are due to Professors Kenneth L. Stevenson (Indiana University – Purdue University at Fort Wayne) and Arnd Vogler (Universität Regensburg) for their generous theoretical and technical help**.** Financial support of this work by the Hungarian Science Foundation (OTKA, No. T035137) is gratefully acknowledged.

References

[1] C.K. Mathews, K.E. van Holde, K.G. Ahern, Biochemistry, Addison Wesley Longman, San Francisco, 2000.
[2] R.H. Garrett, C.M. Grisham, Biochemistry, Saunders College Publishing, Fort Worth, 1999.
[3] G. Knör, A. Strasser, Inorg. Chem. Commun. 8 (2005) 471.
[4] G. Knör, ChemBioChem 2 (2001) 593.
[5] G. Knör, Coord. Chem. Rev. 171 (1998) 61.
[6] D.R. McMillin, Chem. Rev. 98 (1998) 1201.
[7] M.D. Lim, I.M. Lorkovic, P.C. Ford, J. Inorg. Biochem. 99 (2005) 151.
[8] B.O. Fernandez, I.M. Lorkovic, P.C. Ford, Inorg. Chem. 43 (2004) 593.
[9] G.G. Martirosyan, A.S. Azizyan, T.S. Kurtikyan, P.C. Ford, Chem. Commun. (2004) 1488.
[10] P.D. Beer, D.P. Cormode, J.J. Davis, Chem. Commun. (2004) 414.
[11] A. Rest, in: J.D. Coyle, R.R. Hill, D.R. Roberts (Eds.), Light, Chemical Change and Life: A Source Book of Photochemistry, The Open University Press, Walton Hall, 1982, Chapter 2.3.
[12] A. Harriman, J.P. Sauvage, Chem. Soc. Rev. 25 (1996) 41.
[13] I. Scalise, E.N. Durantini, J. Photochem. Photobiol. A: Chem. 162 (2004) 105.
[14] E.S. Nyman, P.H. Hynninen, J. Photochem. Photobiol. B: Biol. 73 (2004) 1.
[15] T.K. Chandrashekar, S. Ganesan, Photochem. Photobiol. 78 (2003) 487.
[16] S.Y. Ma, Chem. Phys. Lett. 332 (2000) 603.
[17] M.F. Hudson, K.M. Smith, Chem. Commun. (1973) 515.
[18] L.L. Wittmer, D. Holten, J. Phys. Chem. 100 (1996) 860.
[19] M. Tabata, M. Tanka, Chem. Commun. (1985) 42.
[20] N.N. Greenwood, A. Earnshaw, Chemistry of the Elements, Pergamon Press, Oxford, 1984.
[21] W. Kaim, B. Schwederski, Bioanorganische Chemie, Teubner-Verlag, Stuttgart, 1992.
[22] A.D. Becke, J. Chem. Phys. 98 (1993) 5648.
[23] C. Lee, W. Yang, R.G. Parr, Phys. Rev. B 37 (1988) 785.
[24] A.D. Becke, Phys. Rev. A 38 (1988) 3098.
[25] M.J. Frisch, G.W. Trucks, H.B. Schlegel, G.E. Scuseria, M.A. Robb, J.R. Cheeseman, V.G. Zakrzewski, J.A. Montgomery Jr., R.E. Stratmann, J.C. Burant, S. Dapprich, J.M. Millam, A.D. Daniels, K.N. Kudin, M.C. Strain, O. Farkas, J. Tomasi, V. Barone, M. Cossi, R. Cammi, B. Mennucci, C. Pomelli, C. Adamo, S. Clifford, J. Ochterski, G.A. Petersson, P.Y. Ayala, Q. Cui, K. Morokuma, N. Rega, P. Salvador, J.J. Dannenberg, D.K. Malick, A.D. Rabuck, K. Raghavachari, J.B. Foresman, J. Cioslowski, J.V. Ortiz, A.G. Baboul, B.B. Stefanov, G. Liu, A. Liashenko, P. Piskorz, I. Komaromi, R. Gomperts, R.L. Martin, D.J. Fox, T. Keith, M.A. Al-Laham, C.Y. Peng, A. Nanayakkara, M. Challacombe, P.M.W. Gill, B. Johnson, W. Chen, M.W. Wong, J.L. Andres, C. Gonzalez, M. Head-Gordon, E.S. Replogle, J.A. Pople, Gaussian 98, Revision A.11.4, Gaussian Inc., Pittsburgh, PA, 2002.
[26] D.F. Shriver, P.W. Atkins, Inorganic Chemistry, Oxford University Press, Oxford, 1999.

[27] J.M. Ugalde, B. Dunietz, A. Dreuw, M. Head-Gordon, R.J. Boyd, J. Phys. Chem. A 106 (2004) 9845.
[28] R. Huszánk, O. Horváth, Chem. Commun. (2005) 224.
[29] Y.Y. Lee, J.H. Chen, H.Y. Hsieh, F.L. Liao, S.L. Wang, J.Y. Tung, S. Elango, Inorg. Chem. Commun. 6 (2003) 252.
[30] J.Y. Tung, J.H. Chen, F.L. Liao, S.L. Wang, L.P. Hwang, Inorg. Chem. 39 (2000) 2120.
[31] K.M. Kadish, A. Tabard, A. Zrineh, M. Ferhat, R. Guilard, Inorg. Chem. 26 (1987) 2459.
[32] J.-J. Lai, S. Khademi, E.F. Meyer Jr., D.L. Cullen, K.M. Smith, J. Porph, Phthalocyanines 5 (2001) 621.
[33] J.M. Okoh, N. Bowles, M. Krishnamurthy, Polyhedron 3 (1984) 1077.
[34] M. Tabata, W. Miyata, N. Nahar, Inorg. Chem. 34 (1995) 6492.
[35] Z. Valicsek, O. Horváth, K.L. Stevenson, Photochem. Photobiol. Sci. 3 (2004) 669.
[36] Z. Valicsek, O. Horváth, submitted for publication.
[37] M. Tabata, K. Ozutsumi, Bull. Chem. Soc. Jpn. 65 (1992) 1438.
[38] A.O. Adeyemo, M. Krishnamurthy, Inorg. Chim. Acta 83 (1984) 41.
[39] O. Horváth, Z. Valicsek, A. Vogler, Inorg. Chem. Commun. 7 (2004) 854.
[40] A. Adeyemo, M. Krishnamurthy, Inorg. Chem. 16 (1977) 3355.
[41] O. Horváth, Z. Valicsek, G. Lendvay, submitted for publication.
[42] M.-C. Wang, L.-S. Sue, B.-C. Liau, B.-T. Ko, S. Elango, J.-H. Chen, Inorg. Chem. 40 (2001) 6064.
[43] O. Horváth, P.C. Ford, A. Vogler, Inorg. Chem. 32 (1993) 2614.
[44] O. Horváth, Z. Valicsek, G. Lendvay, in preparation.